1521-009X/50/8/1077–1086$35.00
DRUG METABOLISM AND DISPOSITION
dx.doi.org/10.1124/dmd.122.000875
Drug Metab Dispos 50:1077–1086, August 2022

Repression of Organic Anion Transporting Polypeptide (OATP) 1B Expression and Increase of Plasma Coproporphyrin Level as Evidence for OATP1B Downregulation in Cynomolgus Monkeys Treated with Chenodeoxycholic Acid[S]

Yueping Zhang, Shen-Jue Chen, Cliff Chen, Xue-Qing Chen, Sagnik Chatterjee, David J. Shuster, Heather Dexter, Laura Armstrong, Elizabeth M. Joshi, Zheng Yang, and Hong Shen

Drug Metabolism and Pharmacokinetics (Y.Z., C.C, E.M.J., Z.Y., H.S.), Discovery Toxicology (S.-J.C., L.A.), Discovery Pharmaceutics (X.-Q.C.), and Veterinary Sciences (D.J.S., H.D.), Bristol Myers Squibb Company, Princeton, New Jersey; and Drug Metabolism and Pharmacokinetics (S.-J.C.), Biocon Bristol Myers Squibb R&D Centre, Syngene International Ltd., Bangalore, India

Received February 21, 2022; accepted May 12, 2022

ABSTRACT

Farnesoid X receptor (FXR) is a nuclear receptor known to markedly alter expression of major transporters and enzymes in the liver. However, its effects toward organic anion transporting polypeptides (OATP) 1B1 and 1B3 remain poorly characterized. Therefore, the present study was aimed at determining the effects of chenodeoxycholic acid (CDCA), a naturally occurring FXR agonist, on OATP1B expression in cynomolgus monkeys. Multiple administrations of 50 and 100 mg/kg of CDCA were first shown to significantly repress mRNA expression of *SLCO1B1/3* approximately 60% to 80% in monkey livers. It also suppressed cytochrome P450 (CYP)7A1-mRNA and induced OSTα/β-mRNA, which are well known targets of FXR and determinants of bile acid homeostasis. CDCA concomitantly decreased OATP1B protein abundance by approximately 60% in monkey liver. In contrast, multiple doses of 15 mg/kg rifampin (RIF), a pregnane X receptor agonist, had no effect on hepatic OATP1B protein, although it induced the intestinal P-glycoprotein and MR2 proteins by ~2-fold. Moreover, multiple doses of CDCA resulted in a steady ~2- to 10-fold increase of the OATP1B biomarkers coproporphyrins (CPs) in the plasma samples collected prior to each CDCA dose. Additionally, 3.4- to 11.2-fold increases of CPI and CPIII areas under the curve were observed after multiple administrations compared with the single dose and vehicle administration dosing groups. Taken together, these data suggest that CDCA represses the expression of OATP1B1 and OATP1B3 in monkeys. Further investigation of OATP1B downregulation by FXR in humans is warranted, as such downregulation effects may be involved in bile acid homeostasis and potential drug interactions in man.

SIGNIFICANCE STATEMENT

Using gene expression and proteomics tools, as well as endogenous biomarker data, for the first time, we have demonstrated that OATP1B expression was suppressed and its activity was reduced in the cynomolgus monkeys following oral administration of 50 and 100 mg/kg/day of chenodeoxycholic acid (CDCA), a Farnesoid X receptor agonist, for 8 days. These results lead to a better understanding of OATP1B downregulation by CDCA and its role on bile acid and drug disposition.

Introduction

Organic anion-transporting polypeptide (OATP)1B1 (*SLCO1B1*) and OATP1B3 (*SLCO1B3*), highly abundant transporters in the liver, represent an efficient route for transporting endogenous and xenobiotic compounds in hepatocytes. It is well established that OATP1B1 and OATP1B3 are high-risk sites of drug-drug interaction in the literature (Niemi, 2007, Niemi et al., 2011, Shitara et al., 2013, Maeda, 2015). For example, an increased plasma concentration of statins and greater

This study was supported by Bristol Myers Squibb Company (Funding from Bristol Myers Squibb Company, Princeton, New Jersey, US).

No author has an actual or perceived conflict of interest with the contents of this article.

dx.doi.org/10.1124/dmd.122.000875.

[S] This article has supplemental material available at dmd.aspetjournals.org.

ABBREVIATIONS: ALA, 5-aminolevulinic acid; ALAS, 5-aminolevulinic acid synthase; *AUC*, area under plasma concentration-time curve; BAAT, bile acid-CoA:amino acid N-acyltransferase; BCRP, breast cancer resistance protein; BSEP, bile salt export pump; CA, cholic acid; CAR, constitutive androstane receptor; CDCA, chenodeoxycholic acid; CYP, cytochrome P450; C_{max}, maximum plasma concentration; CP, coproporphyrin; DCA, deoxycholic acid; FXR, farnesoid X receptor; LCA, lithocholic acid; LC-MS/MS, liquid chromatography–tandem mass spectrometry; LXR, liver X receptor; MDR, multidrug resistance protein; MRP, multidrug resistance-associated protein; NTCP, sodium taurocholate co-transporting polypeptide; OAT, organic anion transporter; OATP, organic anion-transporting polypeptide; OCT, organic cation transporter; OST, organic solute transporter; PCR, polymerase chain reaction; P-gp, P-glycoprotein; PPIA, peptidylprolyl isomerase A; PXR, pregnane X receptor; RIF, rifampicin; RT-PCR, reverse transcription polymerase chain reaction; SHP, small heterodimer partner; UGT, UDP-glucuronosyltransferase.

risk for myopathy and/or rhabdomyolysis occurred in patients who received a co-administration of OATP1B inhibitor gemfibrozil (Backman et al., 2002), or those carrying decreased functional OATP1B1 genetic polymorphism (Parish et al., 2008). It is generally believed that the expression of OATP1B can be regulated by transcriptional, post-transcriptional, and post-translational modification mechanisms, although definitive proof for this assertion has been limited. If true, the activity of OATP1B could be up- or downregulated, and thus could have significant consequences on the systemic exposure to drug substrates, potentially altering the sensitivity or toxicity of certain therapeutic agents. As a result, the United States Food and Drug Administration recommends determining if an investigational drug is an inducer of drug transporters, such as P-glycoprotein (P-gp). Additionally, the European Medicines Agency has recommended that studies should be performed to investigate whether an investigational drug induces and suppresses drug-metabolizing enzymes and drug transporters via modulation of nuclear receptors in addition to direct inhibition. However, the mechanisms of OATP1B1 and OATP1B3 expression remain elusive, and the sciences of transporter regulation continue to be at an early stage.

It has been proposed that a number of nuclear receptors, including pregnane X receptor (PXR), farnesoid X receptor (FXR), liver X receptor alpha (LXRα), constitutive androstane receptor (CAR), and vitamin D receptor are involved in regulation of OATP1B genes (Meyer zu Schwabedissen and Kim, 2009, Eloranta et al., 2012, Alam et al., 2018, Rodrigues et al., 2020), but the investigation of OATP1B regulation, especially downregulation, is limited. Meyer Zu Schwabedissen et al. identified two functional FXR response elements and one LXRα response element in promoting the human *SLCO1B1* gene (Meyer Zu Schwabedissen et al., 2010). The direct interaction between FXR with the identified response elements in *SLCO1B1* gene was then confirmed with chromatin immunoprecipitation assay. Additionally, FXR and LXRα agonists, but not PXR and CAR agonists, were able to induce OATP1B1 in human hepatocytes. Similarly, a response element that binds to FXR was found in the promoter sequence of the human *SLCO1B3* gene (Jung et al., 2002). FXR ligand [chenodeoxycholic acid (CDCA)], but not PXR (clotrimazole) and LXRα ligands (25-hydroxycholesterol), induced OATP1B3 promoter activity. Recently, several putative FXR response elements that were predicted to interact efficiently with FXR were identified in the 5′ untranslated region of both cynomolgus monkey *SLCO1B1* and *SLCO1B3* genes (data not shown), suggesting possible involvement of FXR in modulating monkey OATP1B1 and OATP1B3 expression, although these putative FXR response elements require further validation using functional assays, such as chromatin immunoprecipitation and luciferase activity assays. FXR induces gene transcription by directly binding to a response element in promoters of target genes, such as bile salt export pump (BSEP), and organic solute transporter alpha (OSTα) and beta (OSTβ). However, the binding can suppress human apolipoprotein A-I expression (Claudel et al., 2002). In terms of expression alteration, contradictory effects of the FXR on OATP1B expression have been reported in investigations of differing in vitro models. While ∼4-fold induction of OATP1B1 mRNA was indicative of FXR engagement in cultured human hepatocytes (Meyer Zu Schwabedissen et al., 2010), OATP1B1 mRNA level was repressed ∼2-fold by CDCA in human hepatocytes and liver slices (Jung et al., 2007, Krattinger et al., 2016). In addition, Guo et al. reported that FXR agonist CDCA decreased the uptake clearance of taurocholic acid by ∼2-fold in sandwich-cultured human hepatocytes, whereas the other FXR agonist obeticholic acid showed minimal effect on the uptake clearance (Guo et al., 2018). To our knowledge, there is no in vivo study describing tissue biopsy OATP1B expression profile after multiple administrations of FXR agonists, such as CDCA, in animals and humans. To that end, it is of great interest to investigate the regulatory effects of FXR modulators on OATP1B expression in vivo.

Therefore, the present study was designed to gain insights about the regulation of OATP1B and other transporters by FXR agonist CDCA in vivo, using an in vivo cynomolgus monkey model. Our data indicate that administration of CDCA downregulates OATP1B1 and OATP1B3 expression at mRNA and protein levels after oral administration in monkeys. Such changes may contribute to the alterations of pharmacokinetics in monkeys and humans administered with FXR agonists.

Materials and Methods

Chemicals and Reagents. CDCA, cholic acid (CA), deoxycholic acid (DCA), lithocholic acid (LCA), 5-aminolevulinic acid (ALA), and $^{13}C_5$-^{15}N-ALA were purchased from Sigma Aldrich (St. Louis, MO). CPI and CPIII were obtained from Frontier Scientific (Logan, UT). d4-DCA was purchased from CDN Isotopes (Quebec, Canada). $^{15}N_4$-CPI was purchased from Toronto Research Chemicals (North York, ON, Canada). day$_8$-CPIII was synthesized by Bristol Myers Squibb Company (Princeton, NJ). Formic acid and high-performance liquid chromatography grade methanol, acetonitrile, and water were obtained from Fisher Scientific (Fairlawn, NJ). Bicinchoninic acid protein quantification kits and in-solution trypsin digestion kits were purchased from Pierce (Rockford, IL). The ProteoExtract native membrane protein extraction kit was procured from Calbiochem (San Diego, CA). Synthetic light and heavy peptides for hepatic and intestinal transporter quantification were obtained from New England Peptides (Boston, MA) and Thermo Fisher Scientific (Rockford, IL). Cynomolgus monkey plasma (triple charcoal stripped) for generating plasma calibrators and quality controls (QCs) was obtained from Bioreclamation IVT (Westbury, NY). Unless otherwise noted, all other chemicals were of analytical grade and were from Sigma Aldrich (St. Louis, MO).

Cynomolgus Monkeys Treated with CDCA. All animal protocols were approved by the Institutional Animal Care and Use Committee of Bristol Myers Squibb in accordance with the *Guide for the Care and Use of Laboratory Animals* (Institute of Laboratory Animal Resources, 1996) (https://grants.nih.gov/grants/olaw/guide-for-the-care-and-use-of-laboratory-animals.pdf). Male cynomolgus monkeys (6.8–8.7 kg) were maintained at 22°C on a 12 hours (h): 12 hour light-dark cycle in the Bristol Myers Squibb animal facility (Princeton, NJ). Cynomolgus monkeys were randomized into three groups (vehicle control, 50, and 100 mg/kg of CDCA groups) (n = 3 per group).

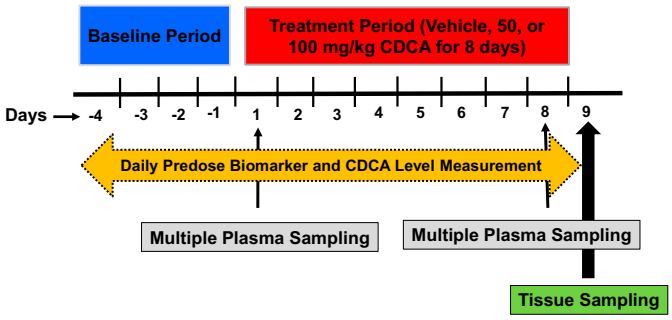

Fig. 1. Schematic diagram of the experimental procedure. Cynomolgus monkeys were orally administered with vehicle or CDCA (50 or 100 mg/kg/d) for 8 consecutive days (n = 3). A single plasma sample was collected for almost every day over an entire study course for measurement of basal endogenous biomarker levels [Predose samples were collected before each CDCA dose during treatment period (i.e., 0 hour)]. In addition, sequential plasma samples were collected from 1, 3, 6, and 24 hours on Day 1 (after the first CDCA dose) and Day 8 (after the eighth CDCA dose) for biomarker and bile acid measurements. Moreover, the liver and proximal jejunum tissue specimens were collected on Day 9 for mRNA expression and proteomics analyses.

During a baseline period (Day -4 through Day -1), blood samples were collected in tubes containing K_2-EDTA at 8:00 AM on Day -4 and Day -1 from all monkeys to determine baseline plasma levels of CPI, CPIII, ALA, and CDCA (Fig. 1). Animals were not fasted for blood sample collections.

From Day 1 to Day 8 (CDCA treatment period), vehicle (0.5% carboxymethyl cellulose), 50, or 100 mg/kg of CDCA were administered once daily for 8 days to three monkeys via oral gavage (Fig. 1). The dose of 50 and 100 mg/kg was selected because previous studies indicated that the administration of 10, 40, and 100 mg/kg of CDCA daily to monkeys for one month resulted in no toxicity and no significant change in liver biopsies (Dyrszka et al., 1975). A single blood sample was collected at 8:00 AM directly before each CDCA or vehicle dose during this period. Additionally, on Day 1 and Day 8, blood samples were collected at 0 (pre-dose), 1, 3, 6, and 24 hours following CDCA administration. Blood samples were stored on wet ice before being centrifuged to obtain plasma [500 xg, 10 minutes (min) at 4°C], and the resultant plasma was stored at −70°C until bioanalysis.

On Day 9, at approximately 24 hours after the last CDCA dose, monkeys were sacrificed, and the liver and small intestine were harvested to allow determination of the effects of CDCA on transporter and enzyme expression after multiple CDCA doses (Fig. 1). For small intestine, approximately the first 4 inches of jejunum (proximal section of jejunum) were excised and perfused with 25 mL of ice-cold saline to remove food contents. The segment was cut lengthwise (4°C), and the intestinal lining was removed by scraping. Tissues were placed immediately in cryotubes and stored at −70°C until analysis.

Reverse Transcription Polymerase Chain Reaction (RT-PCR). The expression of mRNA of OATP1B1, OATP1B3, and other transporters, enzymes, and nuclear receptors in the monkey liver and proximal section of jejunum was determined by real-time RT-PCR assays described previously with slight modifications (Zhang et al., 2020). Briefly, isolation of total RNA from monkey liver and proximal jejunum samples was performed using an RNeasy Mini kit (Qiagen, Valencia, CA) following the manufacturer's instructions. The integrity of the RNA was examined by using an aliquot of the RNA sample on Agilent RNA 6000 Nano chromatin immunoprecipitation. Unfortunately, the RNA of many jejunum samples was degraded as most samples measured RNA Integrade Number <4. As a result, only liver RNA samples were included in RT-PCR analysis. cDNA was produced from 3.3 μg of total RNA by using the SuperScript IV Reverse Transcriptase (Thermo Fisher Scientific, Belmont, CA) in a 40-ul reaction. Real-time quantitative PCR was performed on cDNA samples using a ViiA 7 Real-Time PCR System (Life Technologies, Grand Island, NY) with SYBR Green fluorescence detection. Primer pairs for the transporter, enzyme, and nuclear receptor genes tested, as well as the housekeeping gene encoding peptidylprolyl isomerase A (*PPIA*), are described in Table 1. Gene expression was done using the cycling threshold (Ct) approach. Expression of a target gene was normalized to that of the housekeeping gene (i.e., PPIA gene). While the ΔCt value was calculated by subtracting the Ct value of a target gene from that of PPIA, the ΔΔCt value was determined by subtracting the ΔCt value of vehicle control from that of the CDCA treatment. Gene expression was expressed as a fold change of mRNA level in the sample relative to the vehicle control calculated using the $2^{-\Delta\Delta Ct}$ method.

Targeted Proteomic Quantification of Transporters. Protein expression of hepatic and intestinal uptake and efflux transporters was quantified by quantitative targeted proteomics using the surrogate peptide approach previously described (Cheng et al., 2016).

Approximately 100 mg of cynomolgus monkey liver and proximal jejunum tissue samples were used to isolate membrane fractions using the ProteoExtract Native Membrane Protein Extraction Kit according to the manufacturer's protocol. The final membrane fraction was diluted to a working concentration of 2 μg of membrane protein/μl as quantified by the bicinchoninic acid assay. A total of 200 μg of membrane proteins were reduced, denatured, alkylated, and digested as per our previously reported protocol ($n = 3$) (Qiu et al., 2013). Peptides unique for cynomolgus monkey OATP1B1 (*SLCO1B1*), OATP1B3 (*SLCO1B3*), BCRP (*ABCG2*), BSEP (*ABCB11*), MDR1 (*ABCB1*), MRP2 (*ABCC2*), sodium taurocholate co-transporting polypeptide (NTCP [*SLC10A1*]), and organic cation transporter (OCT1 [*SLC22A1*]), generated by trypsin digestion, were quantified by liquid chromatography–tandem mass spectrometry (LC-MS/MS) (Table 2).

Peptide quantification was conducted on a ABSCIEX 6500 triple quadrupole mass spectrometer (Framingham, MA) coupled to a Shimadzu LC-30A system (Kyoto, Japan) operated in electrospray positive ionization mode.

TABLE 1

Primers and probes used for real-time quantitative RT-PCR in this study

Name	Primer Sequence	Accession No.
ALAS1	GGATCGGGATGGAGTCATGC GGACCGTACCGTGTCAATCA	NM_001285030.1
ALAS2	TGCCCGGGTGTGAGATTTAC AACTTGGCTGCTCCACTGTT	XM_015443623.1
BAAT	AACTATGAAGACCTGCCCGC GGGCCAAAGACCTTCGGATG	XM_005581173.2
BCRP	CGGGTCTGTTGGTCAATCTCA GCTGCAAAGCCGTAAATCCA	XM_015450641.1
CYP3A8	CATGATCAAAACAGTGCTAGTGA AGCAATGACCGTATTCTCTTCCA	NM_001284534.1, XM_015447118.1
CYP7A1	GGAGAAGGCAAACGGGTGAA ATTGGCACCAAATTGCAGCG	XM_005563370.2
FXR	GGAATGTTGGCTGAATGCTTGT TTGTCGAGGTCACTTGTCGC	XM_005571991.2
MDR1 (P-gp)	AGACATGACGGATACCTTTGC AGGCATACCTGGTCATATCTTCC	NM_001287322.1
MRP2	GACTGATAAGAGGCCTCCGC GCCCACCACACCAATCTTCT	NM_001287716.1
MRP3	ACTGTGTGCCCTCATCTTGG GGCCATCTTTGTGAACCACC	XM_005583690.2
MRP4	GTGGGAGCAGGGAAGTCATC CAGTTCCCGAGAACACCCAG	XM_005586096.2
OATP1B1	TGCACTTGGAGGCACCTCAT TGCTCGTATAACCATTGAGTGGA	NM_001284540.1
OATP1B3	TGCTGGGAGTCATAACCATTCC AAATTTGGCAATTCCAACTAAAGAC	NM_001283191.1
OATP1B1/1B3	AAATTGGAAATTTGCTTGTGATTGT GTAATATCCCATGAAGAAATGTGGT	NM_001284540.1, NM_001283191.1
OSTα	CATCGCCTCGTTTTATGCCG CTGTGTGGACCATCATCGGG	XM_005545271.2
OSTβ	CGGCTGTGGTGGTCATGATA GCATCTTTTGTTTTCTGCTTGCC	XM_005559810.2
PPIA	GTCTCCTTCGAGCTGTTTGCA TTCTGTGAAAGCAGGAACCCTT	XM_005550655
SHP	CTCTTCAACCCTGATGTGCC CAGGGCTCCAGGACTTCACA	XM_005544304.2
NTCP	CACGGTTCTCTCTGCCATCA TCGGCACCGTCCATTGAG	NM_001283323.1
UGT1A1	TGGAACCCCACCATCGAATC CGGGTCATTGGGTGACCAAG	NM_001283438.1

Chromatographic separation was achieved using a UPLC Peptide BEH C18 column (1.7 μm, 130 A, 2.1 × 150 mm; Waters, Hertfordshire, UK) at a temperature of 30°C. Peptides were eluted at a flow rate of 300 μl/min, with a gradient mobile phase consisting of 0.1% formic acid in water (A) and 0.1% formic acid in acetonitrile (B). The LC gradient was: (i) 10% B for 0.5 minutes (Zhang et al., 2011), (ii) linear increase from 10% to 30% B in 25 minutes, (iii) linear
increase from 30% to 90% B in 0.5 minutes, (iv) 90% B for 2 minutes, (v) linear decrease from 90% to 10% B in 0.2 minutes, and (vi) 10% B for 2 minutes. The mass spectrometer instrument conditions were set as follows: 5000 V ion spray voltage, 450°C source temperature,40 psi for curtain gas, and 85 and 60 psi for ion source gas #1 and #2, respectively. MS/MS analysis was performed in multiple reactions monitored by detecting the parent to product ion transitions for the surrogate peptides and their respective stable isotope labeled internal standards using optimized instrument parameters listed in Table 2.

Quantification of CPI and CPIII in Plasma and Liver Lysate Samples by LC-MS/MS. The concentrations of CPI and CPIII were measured in all plasma and liver samples collected from the monkey study using LC-MS/MS assays described previously (Zhang et al., 2020).

Quantification of ALA in Plasma by LC-MS/MS. The analysis of ALA was performed on an AB Sciex 5000 QTRAP mass spectrometer (AB Sciex; Foster City, CA) coupled with a Waters Acquity UPLC system (Milford, MA). The chromatographic separation was performed on an Acquity UPLC HSS T3 column (2.1 × 100 mm, 1.8 μm) from Waters (Milford, MA). The system was maintained at 35°C. The mobile phase consisted of two solvents, solvent A (0.1% formic acid in water) and solvent B (methanol). The total run time was 10 minutes, with a flow rate of 0.2 ml per minute (ml/min). The gradient was started at 12% B for 5 minutes, followed by a linear increase to 80% B in 1 minute, and ramp up to 99% B in 0.5 minutes and maintaining 99% B for 1.4 minutes, and then a linear

TABLE 2

Multiple reaction monitoring parameters of peptides selected for targeted analysis of cynomolgus monkey transporters in this study

Transporter	Signature peptide	Parent Ion (z = 2)	Product Ion 1	Product Ion 2	DP (volt)	CE (volt)	RT (min)	On-column Calibration Range (nM)
BCRP	ENLQFSAALR	574.8	664.4	517.4	87	27	17.4	0.156-20
	ENLQFSAAL**R**	579.8	674.4	527.4				
BSEP	STALQLIQ**R**	515.3	841.5	529.3	73	23	16.8	0.078-20
	STALQLIQ**R**	520.3	851.5	539.3				
MDR1	NTTGALT**T**R	467.8	719.4	618.4	77	21	7.65	0.0195-20
	NTTGALTTR	472.8	729.4	628.4				
MRP2	LTIIPQDPIL**F**SGSLR	885.7	665.6	310.1	137	39	26.7	0.156-5
	LTIIPQDPILFSGSL**R**	890.5	670.1	310.1				
NTCP	GIYDGDL**K**	440.7	710.3	547.3	71	17	12.7	0.0195-20
	GIYDGDL**K**	444.7	718.4	555.2				
OATP1B1	LNPIGIA**K**	413.3	598.4	388.3	66	17	14.6	0.0195-20
	LNPIGIA**K**	417.3	606.4	396.3				
OATP1B3	IVQPEL**K**	413.8	614.3	486.3	61	16	12	0.039-20
	IVQPELK	417.8	622.4	494.3				
OCT1	LSPSFA**D**LFR	576.8	855.4	768.4	85	23	24.6	0.039-20
	LSPSFADLF**R**	581.8	865.4	778.4				

DP: declustering potential; CE, collision energy; RT, retention time.
The labeled amino acid residue of the internal standard is shown underlined.

decrease to 12% in 0.1 minutes and maintaining 12% B for 1 minute. The electrospray ionization source was used in the positive ion mode. The LC-MS/MS detector was operated at unit resolution in the multiple reaction monitoring mode using the transitions of the butylated forms of ALA at m/z 188 > 114 and $^{13}C_5$-^{15}N-ALA at m/z 194 > 120 (Zhang et al., 2011). Optimized parameters were as follows: collision gas, curtain gas, gas 1, and gas 2 (nitrogen) 5, 15, 15, and 2 units, respectively, source temperature of 600°C; and ion spray voltage of 4,000 V. The system control and data processing were performed on the AB Sciex Analyst 1.5 software.

Quantification of CDCA, CA, DCA, and LCA in Plasma and Liver Lysate Samples by LC-MS/MS. The plasma and liver concentrations of bile acids, including CDCA, LCA, CA, and DCA, were measured using the same LC-MS/MS methods described previously (Cheng et al., 2017).

Data and Statistic Analyses. The area under the concentration-time curve from time zero to 24 hours [$AUC_{(0\text{-}24h)}$] and maximum plasma concentration (C_{max}) of CPI, CPIII, and CDCA were calculated from plasma concentrations versus time data by performing noncompartmental analysis using Phoenix WinNonlin, version 8.1 (Certara, Princeton, NJ).

Data are reported as mean ± S.D. To test for statistically significant differences among multiple treatments in gene expression and protein abundance for a given transporter, one-way ANOVA was performed. When the F ratio showed that there were significant differences among treatments, the Dunnett method of multiple comparisons was used to determine which treatments differ. Additionally, to test for statistical difference among multiple treatments for $AUC_{(0\text{-}24h)}$ or C_{max}, ANOVA using the Dunnett method for multiple comparisons was performed. All statistical analyses were performed using Prism software (GraphPad Software, Inc., San Diego, CA). Values of $p < 0.05$ were considered to be the minimum level of statistical significance.

Results

CDCA Treatment Repressed Gene Expression of OATP1B in Cynomolgus Monkey Livers. To determine the effect of FXR on OATP1B gene expression, cynomolgus monkeys were administered with 50 and 100 mg/kg of CDCA, as well as the respective vehicle control, daily for 8 days. CYP7A1 that encodes cholesterol 7a hydroxylase, the rate-limiting enzyme in the classic pathway of bile acid synthesis, is a representative target gene of FXR (Goodwin et al., 2000, Kong et al., 2012). CDCA treatment significantly repressed the CYP7A1 mRNA to hardly detectable levels (99.6% to 99.8%) in monkey liver ($p < 0.05$) (Fig. 2 and Table 3). Organic solute transporter (*OST*)α and *OSTβ* are two other representative target genes of FXR (Landrier et al., 2006, Lee et al., 2006). As expected, CDCA treatment induced OSTα and OSTβ expression in cynomolgous monkey liver (10.0- to 678-fold induction) (Fig. 2 and Table 3). However, the differences were not statistically significant due to the large inter-individual variability of OST)α and OSTβ expression in the control group with small sample size ($n = 3$) ($p > 0.05$). Gene expression analysis using primer pairs specific to monkey *SLCO1B1* or *SLCO1B3* gene demonstrated statistically significant suppression of OATP1B1 and OATP1B3 mRNA in the liver (by 55% to 66% and 77% to 80%, respectively) ($p < 0.05$) (Fig. 2 and Table 3). We confirmed the initial observation of OATP1B downregulation by FXR activation by assessing gene expression using a different primer pair with both *SLCO1B1* and *SLCO1B3* genes, in a similar manner. Indeed, daily oral administration of the natural FXR agonist CDCA (50 and 100 mg/kg) showed significantly lower OATP1B1/3 expression in monkey liver on day 8 compared with the vehicle control (mean 0.303- and 0.390-fold changes, respectively; $p < 0.05$) (Fig. 2 and Table 3). These findings indicate that CDCA suppresses OATP1B1 and OATP1B3 expression in cynomolgus monkeys.

We also examined the changes in the expression of other genes involved in bile acid homeostasis and drug metabolism in cynomolgus monkeys after treatment with CDCA (Fig. 2 and Table 3). In detail, CDCA treatment reduced the expression of FXR itself, whereas SHP expression was induced by 50 mg/kg of CDCA. However, due to relatively large inter-animal variability, the changes in SHP mRNA were not considered significant (2.04 ± 0.850- and 1.31 ± 0.530-fold, respectively; $p > 0.05$). As expected, the CYP3A8 and UDP-glucuronosyltransferase (UGT)1A1, described to be PXR target genes (Nishimura et al., 2008, Kim et al., 2010), showed no significant changes at 50 mg/kg of CDCA treatment. A similar pattern was found for bile acid-CoA: amino acid N-acyltransferase (BAAT). CDCA treatment also did not influence the expression of 5-aminolevulinic acid synthase (ALAS)1 and ALAS2, which are the first and rate-limiting enzyme of heme biosynthesis in the liver and erythrocytes, respectively (Ponka, 1999, Hunter and Ferreira, 2009). NTCP, the main bile acid uptake system in hepatocytes known to be downregulated by an FXR-involved pathway in rats but not in mice and humans (Jung et al., 2004) did not show changes in gene expression in monkey liver (Fig. 2 and Table 3). MRP2 was significantly decreased by 50 and 100 mg/kg of CDCA treatment ($p < 0.05$). Breast cancer resistance protein (BCRP) mRNA was also reduced in monkeys administered with 50 and 100 mg/kg of CDCA; however, due to relatively large interindividual variability, the changes were not significant. CDCA

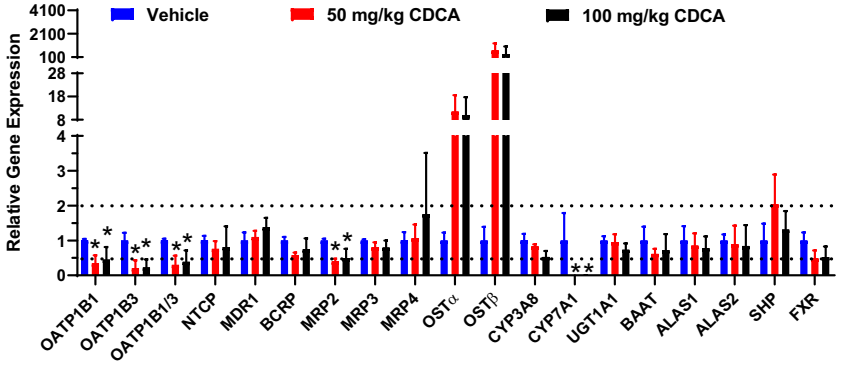

Fig. 2. Relative mRNA expression of transporters, bile acid and enzymes, and nuclear receptors in the liver of cynomolgus monkeys treated with CDCA [50 mg/kg (red bars) and 100 mg/kg (black bars)] once daily for 8 days compared with vehicle control (blue bars). Data are expressed as mean fold-change and SD values from three monkeys. Two lines indicate a 2-fold difference from the vehicle control. Statistics were conducted by ANOVA. *$p < 0.05$ was significantly different compared with vehicle control.

treatment did not influence the gene expression of MDR1 (P-gp), MRP3, and MRP4.

CDCA Treatment Repressed Protein Abundance of OATP1B in Cynomolgus Monkey Livers. In accordance with the mRNA data, chronic treatment with 50 and 100 mg/kg of CDCA was shown to significantly repress protein abundance of OATP1B by approximately 60% in cynomolgus monkey livers ($p < 0.05$) (Fig. 3A and Table 4). Expression of OATP1B1 protein was similar to that of OATP1B3 in control livers (1.59 ± 0.117 and 1.58 ± 0.116 fmol/μg of membrane protein, respectively; $n = 3$). Proteomics analysis clearly showed a reduced protein abundance of OATP1B1 and OATP1B3 in the livers after administration of 50 and 100 mg/kg of CDCA daily for 8 days (0.641 ± 0.322 and 0.580 ± 0.277, and 0.633 ± 0.385 and 0.604 ± 0.372 fmol/μg of membrane protein at doses of 50 and 100 mg/kg, respectively). Additionally, the effect of rifampin (RIF), a PXR agonist, on OATP1B protein abundance was evaluated by analyzing the liver tissue samples from our previous study (Zhang et al., 2020). Administration of 15 mg/kg RIF daily for 7 days had no significant influence on the protein level of OATP1B1 and OATP1B3 in monkey livers compared with controls (1.14 ± 0.276 versus 1.59 ± 0.117, and 0.991 ± 0.162 versus 1.58 ± 0.116 fmol/μg of membrane protein for OATP1B1 and OATP1B3, respectively) ($p > 0.05$) (Fig. 3A), which confirmed absence of OATP1B induction by RIF in cynomolgus monkeys determined using endogenous biomarker and tissue gene expression (Zhang et al., 2020).

BSEP is another representative target gene of FXR. BSEP protein abundance was 5.08 ± 1.16 and 3.32 ± 0.396 fmol/μg of membrane protein in the livers from the monkeys treated with 50 and 100 mg/kg of CDCA, respectively. As expected, the protein abundance values were significantly greater than the values of the control group (1.40 ± 0.246 fmol/μg of membrane protein) (Table 4). The significantly elevated BSEP protein abundance indicates that CDCA activated an FXR pathway in this study. In contrast, RIF had no influence on BSEP protein level in monkey livers compared with the controls (1.57 ± 0.250 fmol/μg of membrane protein). The protein abundance of NTCP, OCT1, and MRP2 was unaltered in the monkey livers treated with CDCA and RIF compared with controls ($p > 0.05$). P-gp protein levels were significantly elevated in the 100 mg/kg CDCA treated monkey livers compared with the control group, but the increase in P-gp protein levels did not reach significance in 50 mg/kg CDCA and 15 mg/kg RIF treatments when compared with control (Table 4). BCRP protein amounts were quite variable in the livers treated with 50 and 100 mg/kg of CDCA and showed no clear trend (Tables 4).

When proximal jejunum tissue examples were examined, statistically significant induction of P-gp and MRP2 protein was observed in monkeys treated with PXR (RIF) but not FXR agonist (CDCA) ($p < 0.05$)

TABLE 3

Effects of CDCA on liver gene expression of transporters, enzymes, and nuclear receptors in cynomolgus monkeys

	50 mg/kg CDCA		100 mg/kg CDCA	
Gene Name	Fold Change (Mean ± SD)	*p*-Value	Fold Change (Mean ± S.D.)	*p*-Value
OATP1B1	0.343 ± 0.233*	0.031	0.450 + 0.360*	0.049
OATP1B3	0.203 ± 0.227*	0.009	0.227 ± 0.231*	0.010
OATP1B1/3	0.303 ± 0.259*	0.021	0.390 ± 0.325*	0.037
NTCP	0.763 ± 0.217	0.666	0.813 ± 0.595	0.768
MDR1	1.10 ± 0.174	0.808	1.38 ± 0.269	0.147
BCRP	0.580 ± 0.072	0.068	1.743 ± 0.316	0.262
MRP2	0.400 ± 0.078*	0.007	0.500 ± 0.261*	0.015
MRP3	0.810 ± 0.135	0.245	0.797 ± 0.200	0.211
MRP4	1.067 ± 0.393	0.996	01760 ± 1.75	0.605
OSTα	11.6 ± 7.03	0.128	10.0 ± 7.70	0.193
OSTβ	678 ± 596	0.248	376 ± 638	0.591
CYP3A8	0.833 ± 0.057	0.335	0.530 ± 0.168	0.054
CYP7A1	0.002 ± 0.001*	0.042	0.004 ± 0.003*	0.043
UGT1A1	0.957 ± 0.224	0.939	0.737 ± 0.179	0.204
BAAT	0.617 ± 0.146	0.381	0.723 ± 0.460	0.573
ALAS1	0.853 ± 0.354	0.672	0.783 ± 0.332	0.524
ALAS2	0.893 ± 0.536	0.947	0.843 ± 0.601	0.891
SHP	2.04 ± 0.850	0.158	1.31 ± 0.530	0.783
FXR	0.490 ± 0.227	0.088	0.523 ± 0.306	0.108

Statistics were conducted by one-way ANOVA followed by Dunnett's multiple comparison. *$p < 0.05$ compared with the vehicle group.

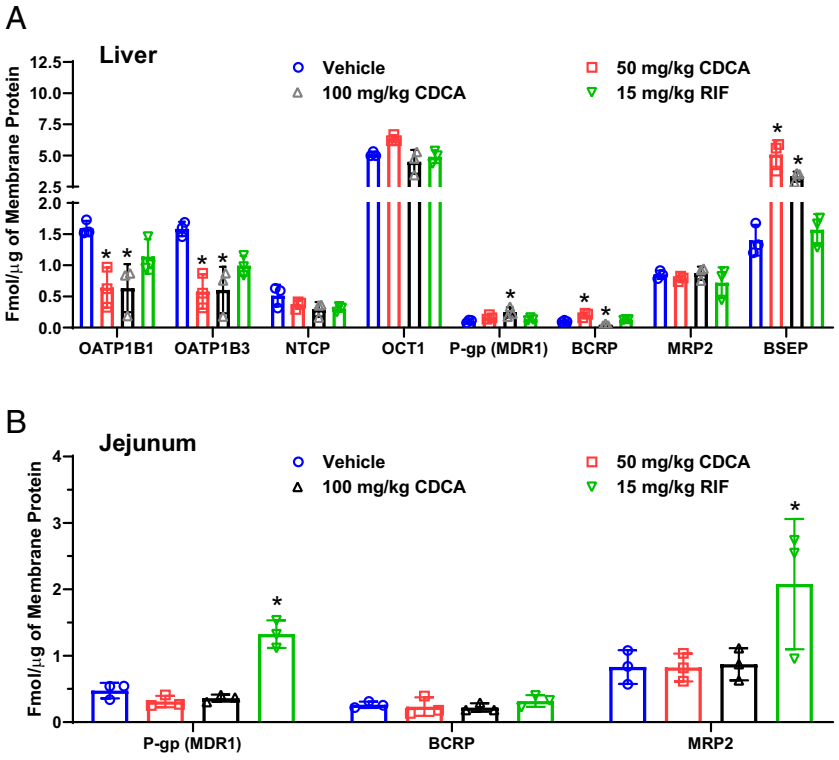

Fig. 3. Abundance of transporter proteins in the liver (A) and proximal jejunum (B) of cynomolgus monkeys treated with vehicle (blue bars), CDCA (50 and 100 mg/kg; red and black bars, respectively), or RIF (15 mg/kg; green bars) once daily for 7 to 8 days. Data are expressed as mean and SD values from three to seven monkeys per group. Statistics were conducted by ANOVA. *$p < 0.05$ was significantly different compared with vehicle controls.

(Fig. 3B and Table 4). RIF was also able to mediate a 1.2-fold increase in BCRP protein (Fig. 3B and Table 4), but the difference did not reach significance because of considerable variation in protein level.

CDCA Treatment Increased Baseline Plasma Levels of CPI and CPIII in Cynomolgus Monkeys. To confirm that the observed suppression in OATP1B1 and OATP1B3 mRNA and protein expression is reflected as functional transport activity, the effect of CDCA treatment on plasma levels of CPI and CPIII in cynomolgus monkeys was evaluated, which were recently characterized as functional biomarkers of OATP1B1 and OATP1B3 (Shen et al., 2016). The daily CDCA treatment was started on Day 1 and terminated on Day 8, and the plasma concentrations of CPI, CPIII, and bile acids were determined 4 days before, during the CDCA treatment, and 1 day thereafter for all monkeys (Fig. 1). The results of plasma concentrations of CPI, CPIII, and bile acids, following single and multiple doses of 50 and 100 mg/kg of CDCA to cynomolgus monkeys, are presented in Figs. 4, 5, and 6, Supplemental Fig. 1, and Table 5. The mean baseline plasma concentrations of CPI and CPIII were 2.55 ± 0.547 and 0.941 ± 0.339 nM on Day -4 (4 days before the first dose of CDCA), and 2.50 ± 0.397 and 0.790 ± 0.329 nM on Day -2, respectively (Figs. 4A and 4B), which are similar to those reported by our group previously (Zhang et al., 2020). Additionally, while the basal plasma CPI concentrations in the monkeys administered with vehicle remained unaltered throughout the whole study, those of 50 and 100 mg/kg of CDCA, determined as the ones prior to CDCA administration for each morning during the CDCA treatment period, exhibited a steady rise in plasma CPI concentration starting from the third dose on Day 4 (4.65 ± 2.28 and 6.93 ± 8.99 nM, respectively) to Day 8 (12.6 ± 7.01 and 5.12 ± 3.27 nM, respectively) (~2- to 5-fold increases compared with before dosing and vehicle control). There was no change in the CPI level after the first and second doses of CDCA on Day 2 and Day 3, respectively (Fig. 4A). Similar to CPI, the 50 and 100 mg/kg CDCA provoked 8.9- and 10.5-fold increases in basal

TABLE 4

Effect of CDCA and RIF on protein expression of liver and jejunum transporters in cynomolgus monkeys

Transporter	Vehicle fmol/μg protein	50 mg/kg CDCA fmol/μg protein	50 mg/kg CDCA *p*-value	100 mg/kg CDCA fmol/μg protein	100 mg/kg CDCA *p*-value	15 mg/kg RIF fmol/μg protein	15 mg/kg RIF *p*-value
OATP1B1	1.59 ± 0.117	0.641 ± 0.322*	0.010	0.633 ± 0.385*	0.010	1.14 +0.276	0.213
OATP1B3	1.58 ± 0.116	0.580 ± 277*	0.003	0.604 ± 0.372*	0.004	0.991 ± 0.162	0.051
NTCP	0.512 ± 0.173	0.366 ± 0.066	0.315	0.294 ± 0.116	0.103	0.302 ± 0.046	0.115
OCT1	5.10 ± 0.195	6.35 ± 0.281	0.067	4.49 ± 0.959	0.462	4.90 ± 0.512	0.948
P-gp (MDR1)	0.104 ± 0.024	0.166 ± 0.036	0.325	0.244 ± 0.081*	0.018	1.14 ± 0.024	0.765
BCRP	0.102 ± 0.013	0.201 ± 0.039*	0.002	0.044 ± 0.016*	0.033	0.127 ± 0.007	0.413
MRP2	0.850 ± 0.064	0.786 ± 0.044	0.894	0.874 ± 0.105	0.993	0.721 ± 0.244	0.556
BSEP	1.40 ± 0.246	5.08 ± 1.16*	0.000	3.32 ± 0.396*	0.016	1.57 ± 0.250	0.976
P-gp (MDR1)	0.475 ± 0.117	0.310 ± 0.086	0.338	0.361 ± 0.054	0.599	1.33 ± 0.208*	0.000
BCRP	0.261 ± 0.047	0.234 ± 0.140	0.967	0.220 ± 0.063	0.904	0.318 ± 0.089	0.795
MRP2	0.830 ± 0.255	0.823 ± 0.210	>0.9999	0.873 ± 0.242	0.999	2.08 ± 0.980*	0.049

Statistics were conducted by one-way ANOVA followed by Dunnett's multiple comparison method. *$p < 0.05$ compared with the vehicle group.

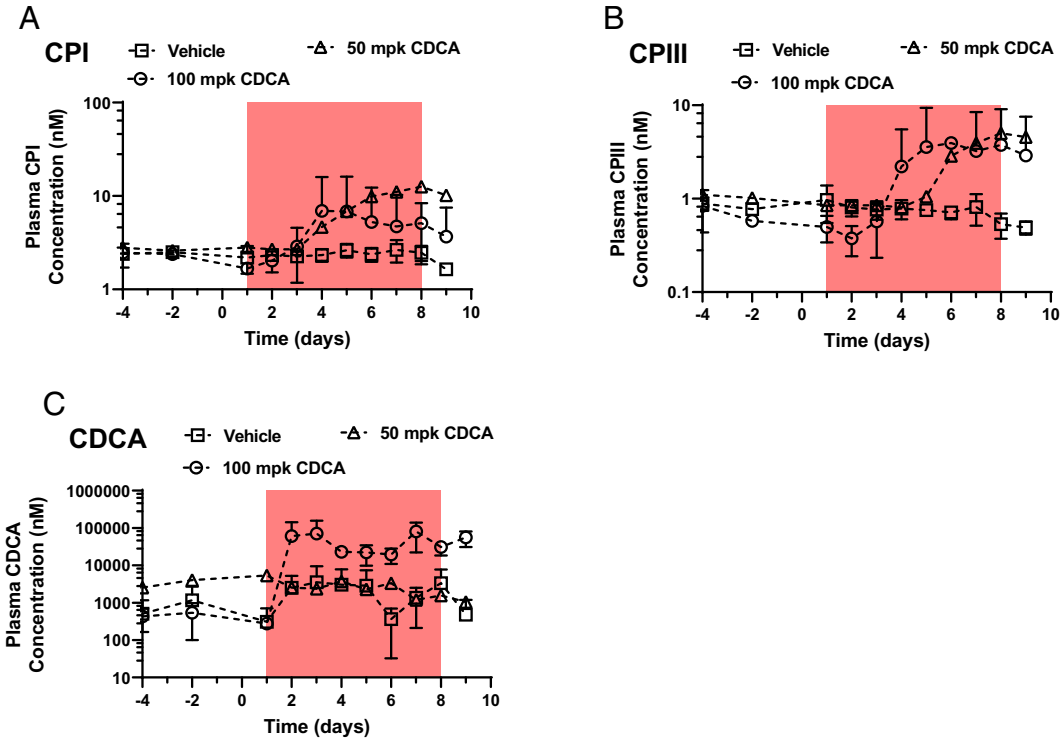

Fig. 4. Mean basal plasma concentrations of CPI (A), CPIII (B), and CDCA (C) in cynomolgus monkeys before (Day -4 and Day -2), during (Day 1 to Day 8), and one day after (Day 9) administration of CDCA (50 and 100 mg/kg/d). Data are shown as the mean and S.D. values.

plasma CPIII concentration, respectively (Fig. 4B). There is considerable variation in baseline plasma CDCA levels in monkeys (~40-fold), and the basal CDCA concentration (trough concentration) was increased > 50-fold in monkeys treated with 100 mg/kg of CDCA during the entire CDCA treatment period (i.e., from Day 2 to Day 8) compared with before dosing and vehicle control (Fig. 4C). In contrast, the basal plasma CDCA concentrations showed relatively constant levels in the monkeys treated with the low CDCA dose. Plasma concentrations of other unconjugated bile acids were also measured in cynomolgus monkeys (Supplemental Fig. 1). Basal plasma concentration of LCA, a bile acid formed from CDCA by bacterial action, was elevated ~10-fold in CDCA-treated monkeys compared with the control, whereas those of CA and DCA were widely varied and unchanged between groups (Supplemental Fig. 1).

We further evaluated the effects of single versus multiple doses of CDCA on plasma concentrations of CPI and CPIII. As shown in Fig. 5 and Table 5, a single dose of 50 or 100 mg/kg of CDCA had no apparent effect on plasma CP concentrations with less than 1.4-fold increase in $AUC_{0\text{-}24h}$ of CPI and CPIII (Table 5). However, multiple doses of both 50 and 100 mg/kg of CDCA markedly increased the plasma CPI and CPIII concentrations compared with control (209 ± 174 and 151 ± 76.6 versus 44.5 ± 2.5 nM·h, and 146 ± 108 and 91.0 ± 116 versus 13.6 ± 2.1 nM·h for CPI and CPIII $AUC_{0\text{-}24h}$, respectively) (Table 5), suggesting altered elimination and/or synthesis of CPI and CPIII. In addition, the plasma CPI-to-ALA and CPIII-to-ALA concentration ratios shared the same profiles with the plasma CPI and CPIII concentrations, indicating limited effects on CP synthesis by chronic CDCA treatment in the monkeys (Figs. 5C and 5D). Both single- and multiple-dose CDCA administration produced a dose-related increase in plasma CDCA concentration (~3- and 80-fold increases in CDCA $AUC_{0\text{-}24h}$ at 50 and 100 mg/kg of CDCA, respectively), while no measurable effect on the plasma levels of LCA, CA, and DCA was observed (Fig. 6, Supplemental Fig. 2, and Table 5). Approximately 3- and 80-fold increases in plasma CDCA concentration but no increase in the CP levels following a single dose of 50 and 100 mg/kg of CDCA on Day 1 indicate that CDCA had no inhibitory effect on monkey OATP1B activity in vivo.

Subsequently, we assessed for the effects of the CDCA and RIF treatments on the monkey liver concentrations of the endogenous biomarker and bile acids (Supplemental Fig. 3). Measurement revealed no apparent liver accumulation of CPI, CPIII, and CDCA after chronic treatments with FXR or PXR agonist, respectively. Interestingly, there was a trend of increased liver LCA concentration in monkeys treated with CDCA (Supplemental Fig. 3D).

Discussion

In this evaluation using a cynomolgus monkey model for OATP1B transporters, for the first time, we provide in vivo evidence of the downregulation of OATP1B via the FXR agonist CDCA via the following observations: (1) suppression of OATP1B1 and OATP1B3 mRNA levels, (2) repression of OATP1B1 and OATP1B3 protein abundance, and (3) blocking OATP1B activity as reflected with increased plasma levels of endogenous biomarkers CPI and CPIII following multiple administrations of CDCA. Altogether, we present the role of the FXR in regulating *SLCO1B* expression.

As a non-steroid hormone nuclear receptor, FXR binds to specific DNA response elements of target genes as a heterodimeric complex with the retinoid X receptor, and modulates the transcription of the genes (Edwards et al., 2002, Claudel et al., 2005). Given that functional FXR response elements have been identified in the 5′ untranslated region of human *SLCO1B1* and *SLCO1B3* genes (Jung et al., 2002, Meyer Zu Schwabedissen et al., 2010), and previous studies have suggested OATP1B expression suppression is a part of the FXR-mediated protection against liver injury induced by cytotoxic bile acids (Geier

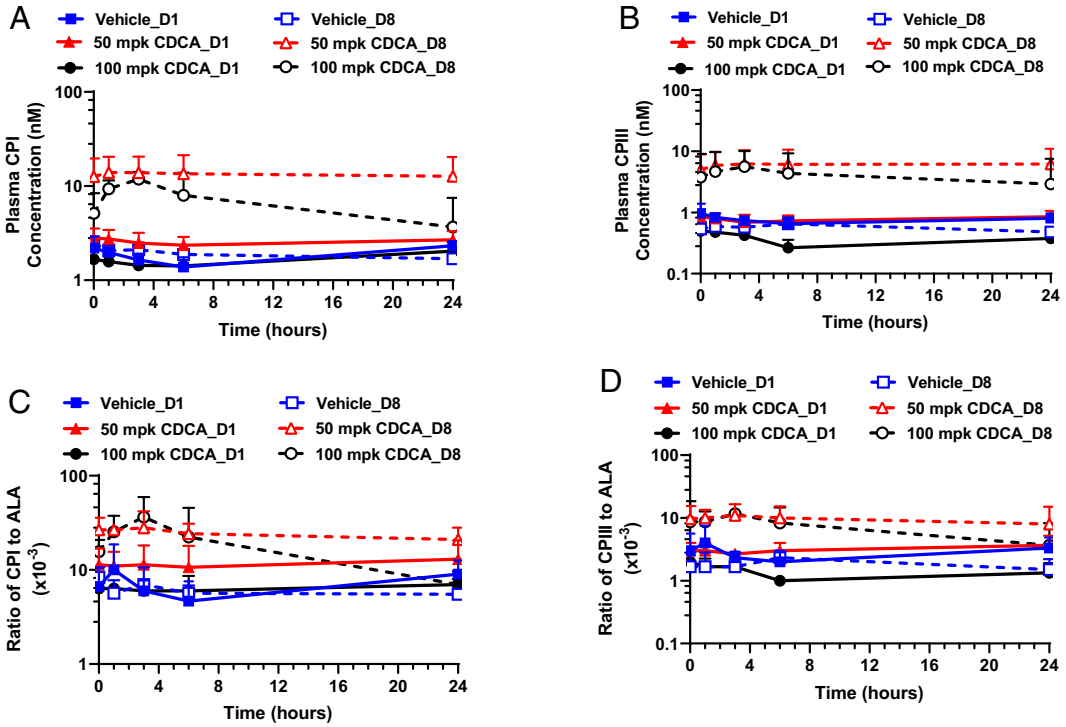

Fig. 5. Mean plasma concentrations of CPI (A), CPIII (B), ratios of CPI to ALA (C), and ratios of CPIII to ALA (D) on Day 1 after the first vehicle (blue closed squares), 50 mg/kg (mpk) of CDCA (red closed triangles), or 100 mpk of CDCA dose (black closed circles), and on Day 8 after the eighth vehicle (blue open squares), 50 mpk of CDCA (red open triangles), or 100 mpk of CDCA dose (black open circles) are shown as mean and S.D. values. Pharmacokinetics are summarized in Table 5.

et al., 2007), we hypothesized that FXR activation in the liver downregulates OATP1B expression, thereby impairing OATP1B-mediated uptake of endogenous substrates and drugs in hepatocytes. To test this hypothesis, we first determined whether the cynomolgus monkey model retained for our study was suitable for evaluating the effects of CDCA, the most potent and established natural FXR ligand, on OATP1B expression when used at the doses of 50 and 100 mg/kg, which were previously shown to be nontoxic to monkeys as determined by blood test and histology assay (Dyrszka et al., 1975). For this purpose, we analyzed expression of referent gene expression markers, such as *CYP7A1*, *OSTα*, and *OSTβ*, well known targets of FXR (Goodwin et al., 2000, Landrier et al., 2006, Lee et al., 2006, Kong et al., 2012, van de Wiel et al., 2019). As shown in Fig. 2 and Table 3, both 50 and 100 mg/kg CDCA treatments for 8 days were able to highly suppress CYP7A1 mRNA expression and induce OSTα, and OSTβ mRNA levels in monkeys, although there was a lack of dose-dependent modulation. This indicated that these monkeys were responsive to altered bile acid levels and thus were suitable for investigating FXR effects toward OATP1B expression in vivo.

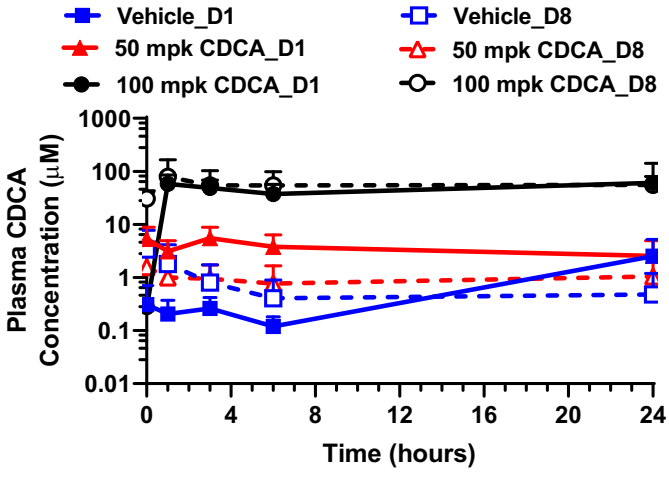

Fig. 6. Mean plasma concentrations of CDCA on Day 1 after the first vehicle (blue closed squares), 50 mpk of CDCA (red closed triangles), or 100 mpk of CDCA dose (black closed circles), and on Day 8 after the eighth vehicle (blue open squares), 50 mpk of CDCA (red open triangles), or 100 mpk of CDCA dose (black open circles) are shown as mean and S.D. values. CDCA pharmacokinetics are summarized in Table 5.

We subsequently analyzed OATP1B1 and OATP1B3 expression in CDCA-treated cynomolgus monkeys. Analysis of mRNA expression using quantitative RT-PCR (Fig. 2 and Table 3) indicated that chronic CDCA treatment repressed 55% and 80% of OATP1B1 and OATP1B3 mRNA in monkey livers, fully supporting that OATP1B is downregulated by the FXR agonist in cynomolgus monkeys. CDCA treatment was also found to downregulate OATP1B protein levels, as determined by targeted proteomics analysis, in monkey livers (Fig. 3 and Table 4). Thus, protein OATP1B abundance was markedly repressed in response to an 8-day CDCA treatment, by a 2.5- to 2.7-fold factor in OATP1B1 and OATP1B3 protein levels. This observation is consistent with the significantly decreased *SLCO1B1* promoter activity in hepatoma cells and reduced OATP1B1 expression in human liver slices induced by CDCA (Jung and Kullak-Ublick, 2003, Jung et al., 2007). In addition, this finding is also in agreement with the observations that OATP1B expression is negatively correlated with bile acid levels in patients with cholestatic liver diseases as an early defense mechanism for hepatocytes to shut off bile acid influx (Oswald et al., 2001, Zollner et al., 2001, Keitel et al., 2005). In contrast, a 7-day RIF treatment had a limited effect (slight repression but not induction) on OATP1B1 and OATP1B3 protein levels in monkey liver, although significant induction of P-gp and MRP2 protein levels in monkey intestine were seen ($p < 0.05$)

TABLE 5

Systemic exposures of CPI, CPIII, and CDCA after the first and multiple administrations of CDCA to cynomolgus monkeys (Day 1 and Day 8, respectively).

		Vehicle Control		50 mg/kg CDCA		100 mg/kg CDCA	
Analyte	Exposure	Day 1	Day 8	Day 1	Day 8	Day 1	Day 8
CPI	$AUC_{0\text{-}24h}$ (nM·h)	43.5 ± 6.3	44.5 ± 2.5	60.6 ± 14.3	209 ± 174	39.9 ± 11.9	151 ± 76.6
	C_{max} (nM)	2.5 ± 0.44	2.5 ± 0.44	2.8 ± 0.74	14.2 ± 6.7*	2.1 ± 0.48	11.9 ± 2.3*
CPIII	$AUC_{0\text{-}24h}$ (nM·h)	17.6 ± 3.5	13.6 ± 2.1	18.6 ± 3.8	146 ± 108	8.1 ± 2.3	91.0 ± 116
	C_{max} (nM)	1.0 ± 0.36	0.68 ± 0.18	0.90 ± 0.17	6.7 ± 4.4	0.50 ± 0.16	5.6 ± 4.5
CDCA	$AUC_{0\text{-}24h}$ (μM·h)	25.0 ± 25.5	14.6 ± 19.3	82.4 ± 60.5	21.9 ± 25.3	1132 ± 942*	1308 ± 540*
	C_{max} (μM)	2.5 ± 2.7	3.4 ± 4.4	6.6 ± 2.9	2.0 ± 1.7	96.2 ± 55.5*	102 ± 68.0*

Data represent the mean and S.D. from 3 monkeys; $AUC_{(0\text{-}24h)}$, area under plasma concentration-time curve from time 0 to 24 h; C_{max}, maximum plasma concentration. Statistics were conducted using one-way ANOVA followed by Dunnett's multiple comparison method. *$p < 0.05$ compared with the first vehicle dose (Day 1).

(Fig. 3 and Table 4), suggesting that expression of both OATP1Bs in monkey liver was unaltered by the PXR agonist. Similar observations have been reported for human subjects, where there was no significant modulation of OATP1B protein expression by RIF, as assessed by serum-derived small extracellular vesicles (Rodrigues et al., 2021).

We next studied the day-to-day change from basal pre-dose plasma levels throughout the entire study treated with CDCA. The FXR activator was found to markedly increase basal pre-dose plasma CPI and CPIII levels in cynomolgus monkeys (Fig. 4), which are observed endogenous substrates of monkey and human OATP1B transporters (Lai et al., 2016, Shen et al., 2016). This bile acid also markedly increased the plasma concentrations of CPI and CPIII, endogenous probes of OATP1B, following multiple doses of CDCA on Day 8 compared with the single dose on Day 1 (Fig. 5). These results suggest that OATP1B activity was repressed by CDCA. The complexity of underlying mechanisms for increased basal plasma CPI and CPIII levels is reflected in the data from a study by Peyer et al., who found that ALAS1 mRNA activity is increased upon exposure to CDCA in human hepatocytes and liver slices (Peyer et al., 2007). CDCA had no effect on the mRNA levels of ALAS1 and ALAS2, the rate-limiting enzymes of heme biosynthesis in the body, in monkeys (Fig. 2 and Table 3). Additionally, the observed strong increases of the ratio of CP to ALA after multiple doses of CDCA compared with the single dose indicate limited or no effects of CDCA on CP synthesis in monkeys (Fig. 5). Beyond considering CP synthesis induction, it is tempting to speculate about OATP1B inhibition as a mechanism of elevated CP levels since the it has been reported that CDCA is an in vitro inhibitor of human OATP1B1 with an inhibition constant of 3.4 ± 0.5 μM (Gui et al., 2009). However, the fact that the basal plasma CP levels started increasing on Day 4 but not Day 1 (Fig. 4), and the plasma concentrations of CP following a single dose of 50 and 100 mg/kg of CDCA were similar to those of vehicle control (Fig. 5), indicating that OATP1B inhibition is not a factor in increasing the concentrations of the endogenous biomarkers in this study. Taken together, these data establish that OATP1B expression is markedly suppressed in response to CDCA in monkey livers.

Although we demonstrated that CDCA suppressed OATP1B expression and reduced OATP1B activity in cynomolgus monkeys, additional studies may be needed to identify the mechanisms and signaling pathways of OATP1B gene suppression that follow binding of CDCA to FXR. CDCA can activate FXR, and then induce SHP that functions to mainly suppress gene expression of CYP7A in the liver (Goodwin et al., 2000, Lu et al., 2000). We showed that 50 and 100 mg/kg CDCA increased the SHP mRNA levels by 2- and 1.3-fold compared with the control in monkey liver (Fig. 2 and Table 3). Although the increases are smaller than the common increases of SHP induced by FXR agonists in liver cells and tissues (~3-fold) (Qin et al., 2005, Jung et al., 2007), the increased SHP concentrations may further suppress OATP1B expression. In addition, FXR can induce fibroblast growth factor 19 (FGF19) in cynomolgus monkeys and humans and FGF15 in mice in small intestine. The FGF19/15 circulate back to hepatocytes via portal vein and activate fibroblast growth factor receptor 4-βklotho complex in hepatocytes, leading to activation of the extracellular signal-regulated kinase 1/2 and c-Jun N-terminal kinase 1/2 pathways to suppress the expression of genes, such as CYP7A1, OATP1B, and NTCP (Inagaki et al., 2005, Song et al., 2009, Pai et al., 2012, Slijepcevic et al., 2017). Two out of three monkeys administered with 50 mg/kg of CDCA and one out of three animals administered with 100 mg/kg of CDCA displayed high bilirubin levels in this study (data not shown). It is possible that OATP1B expression is repressed by immunoinflammatory cytokines, such as interleukin-1β, necrosis factor, and interleukin-6 (Jung and Kullak-Ublick, 2003, Le Vee et al., 2008, Le Vee et al., 2009).

In conclusion, for the first time, our results indicate that expression of OATP1B1 and OATP1B3, as measured by the mRNA and protein levels, were decreased in cynomolgus monkeys chronically treated with FXR agonist CDCA. Decreased OATP1B expression explains the marked increases of plasma CPI and CPIII levels after multiple administration of CDCA compared with the single dose and vehicle control, as well as the baseline level before dosing. Downregulation of OATP1B might be a consequence of FXR activation and could serve to block the hepatic uptake of drug substrates, resulting in increased systemic drug exposures. However, further investigations to assess OATP1B downregulation in humans using FXR agonists are required. Several FXR agonists (e.g., obeticholic acid) are in development for the treatments of cardiometabolic diseases. Regulation of OATP1B by these FXR agonists can be further evaluated in human subjects, which are poorly characterized in terms of their regulation effect on drug transporters and their role in drug-drug interaction. In addition, interspecies differences in the functions of FXR need be considered. It is known that FXR activation also takes place during cholestasis disorders, which may lead to an increase in CP concentrations. This may explain a potential for CPs as biomarkers in cases of drug-induced cholestasis and associated liver injury.

Acknowledgments

The authors thank Dr. Kurex Sidik (Biostatistics Department at Bristol Myers Squibb) for his assistance on the statistical analysis of the cynomolgus monkey gene expression, protein abundance, and pharmacokinetics data. In addition, the authors thank Dr. Grace L. Guo (Department of Pharmacology and Toxicology, Ernest Mario School of Pharmacy, Rutgers University, Piscataway, NJ) for performing in silico scan for DNA binding motifs of nuclear receptors.

Authorship Contributions

Participated in research design: Zhang, S.-J. Chen, Armstrong, Joshi, Yang, Shen.

Conducted experiments: Zhang, S.-J. Chen., C. Chen, X.-Q. Chen, Shuster, Dexter.

Contributed new reagents or analytic tools: Zhang, S.-J. Chen, Shen.

Performed data analysis: Zhang, S.-J. Chen, C. Chen, Shen.

Wrote or contributed to the writing of the manuscript: Zhang, S.-J. Chen, C. Chen, Chatterjee, Shen.

References

Alam K, Crowe A, Wang X, Zhang P, Ding K, Li L, and Yue W (2018) Regulation of Organic Anion Transporting Polypeptides (OATP) 1B1- and OATP1B3-Mediated Transport: An Updated Review in the Context of OATP-Mediated Drug-Drug Interactions. *Int J Mol Sci* **19**:855.

Backman JT, Kyrklund C, Neuvonen M, and Neuvonen PJ (2002) Gemfibrozil greatly increases plasma concentrations of cerivastatin. *Clin Pharmacol Ther* **72**:685–691.

Cheng Y, Chen S, Freeden C, Chen W, Zhang Y, Abraham P, Nelson DM, Humphreys WG, Gan J, and Lai Y (2017) Bile Salt Homeostasis in Normal and Bsep Gene Knockout Rats with Single and Repeated Doses of Troglitazone. *J Pharmacol Exp Ther* **362**:385–394.

Cheng Y, Freeden C, Zhang Y, Abraham P, Shen H, Wescott D, Humphreys WG, Gan J, and Lai Y (2016) Biliary excretion of pravastatin and taurocholate in rats with bile salt export pump (Bsep) impairment. *Biopharm Drug Dispos* **37**:276–286.

Claudel T, Staels B, and Kuipers F (2005) The Farnesoid X receptor: a molecular link between bile acid and lipid and glucose metabolism. *Arterioscler Thromb Vasc Biol* **25**:2020–2030.

Claudel T, Sturm E, Duez H, Torra IP, Sirvent A, Kosykh V, Fruchart JC, Dallongeville J, Hum DW, Kuipers F, et al. (2002) Bile acid-activated nuclear receptor FXR suppresses apolipoprotein A-I transcription via a negative FXR response element. *J Clin Invest* **109**:961–971.

Dyrszka H, Chen T, Salen G, and Mosbach EH (1975) Toxicity of chenodeoxycholic acid in the rhesus monkey. *Gastroenterology* **69**:333–337.

Edwards PA, Kast HR, and Anisfeld AM (2002) BAREing it all: the adoption of LXR and FXR and their roles in lipid homeostasis. *J Lipid Res* **43**:2–12.

Eloranta JJ, Hiller C, Jüttner M, and Kullak-Ublick GA (2012) The SLCO1A2 gene, encoding human organic anion-transporting polypeptide 1A2, is transactivated by the vitamin D receptor. *Mol Pharmacol* **82**:37–46.

Geier A, Wagner M, Dietrich CG, and Trauner M (2007) Principles of hepatic organic anion transporter regulation during cholestasis, inflammation and liver regeneration. *Biochim Biophys Acta* **1773**:283–308.

Goodwin B, Jones SA, Price RR, Watson MA, McKee DD, Moore LB, Galardi C, Wilson JG, Lewis MC, Roth ME et al. (2000) A regulatory cascade of the nuclear receptors FXR, SHP-1, and LRH-1 represses bile acid biosynthesis. *Mol Cell* **6**:517–526.

Parish S, Armitage J, Bowman L, Heath S, Matsuda F, Gut I, Lathrop M, Collins R, and Collins R; SEARCH Collaborative Group (2008) SLCO1B1 variants and statin-induced myopathy–a genomewide study. *N Engl J Med* **359**:789–799.

Gui C, Wahlgren B, Lushington GH, and Hagenbuch B (2009) Identification, Ki determination and CoMFA analysis of nuclear receptor ligands as competitive inhibitors of OATP1B1-mediated estradiol-17beta-glucuronide transport. *Pharmacol Res* **60**:50–56.

Guo C, LaCerte C, Edwards JE, Brouwer KR, and Brouwer KLR (2018) Farnesoid X Receptor Agonists Obeticholic Acid and Chenodeoxycholic Acid Increase Bile Acid Efflux in Sandwich-Cultured Human Hepatocytes: Functional Evidence and Mechanisms. *J Pharmacol Exp Ther* **365**:413–421.

Hunter GA and Ferreira GC (2009) 5-aminolevulinate synthase: catalysis of the first step of heme biosynthesis. *Cell Mol Biol* **55**:102–110.

Inagaki T, Choi M, Moschetta A, Peng L, Cummins CL, McDonald JG, Luo G, Jones SA, Goodwin B, Richardson JA, et al. (2005) Fibroblast growth factor 15 functions as an enterohepatic signal to regulate bile acid homeostasis. *Cell Metab* **2**:217–225.

Jung D, Elferink MG, Stellaard F, and Groothuis GM (2007) Analysis of bile acid-induced regulation of FXR target genes in human liver slices. *Liver Int* **27**:137–144.

Jung D, Hagenbuch B, Fried M, Meier PJ, and Kullak-Ublick GA (2004) Role of liver-enriched transcription factors and nuclear receptors in regulating the human, mouse, and rat NTCP gene. *Am J Physiol Gastrointest Liver Physiol* **286**:G752–G761.

Jung D and Kullak-Ublick GA (2003) Hepatocyte nuclear factor 1 alpha: a key mediator of the effect of bile acids on gene expression. *Hepatology* **37**:622–631.

Jung D, Podvinec M, Meyer UA, Mangelsdorf DJ, Fried M, Meier PJ, and Kullak-Ublick GA (2002) Human organic anion transporting polypeptide 8 promoter is transactivated by the farnesoid X receptor/bile acid receptor. *Gastroenterology* **122**:1954–1966.

Keitel V, Burdelski M, Warskulat U, Kühlkamp T, Keppler D, Häussinger D, and Kubitz R (2005) Expression and localization of hepatobiliary transport proteins in progressive familial intrahepatic cholestasis. *Hepatology* **41**:1160–1172.

Kim S, Dinchuk JE, Anthony MN, Orcutt T, Zoeckler ME, Sauer MB, Mosure KW, Vuppugalla R, Grace Jr JE, Simmermacher J, et al. (2010) Evaluation of cynomolgus monkey pregnane X receptor, primary hepatocyte, and in vivo pharmacokinetic changes in predicting human CYP3A4 induction. *Drug Metab Dispos* **38**:16–24.

Kong B, Wang L, Chiang JY, Zhang Y, Klaassen CD, and Guo GL (2012) Mechanism of tissue-specific farnesoid X receptor in suppressing the expression of genes in bile-acid synthesis in mice. *Hepatology* **56**:1034–1043.

Krattinger R, Boström A, Lee SML, Thasler WE, Schiöth HB, Kullak-Ublick GA, and Mwinyi J (2016) Chenodeoxycholic acid significantly impacts the expression of miRNAs and genes involved in lipid, bile acid and drug metabolism in human hepatocytes. *Life Sci* **156**:47–56.

Lai Y, Mandlekar S, Shen H, Holenarsipur VK, Langish R, Rajanna P, Murugesan S, Gaud N, Selvam S, Date O, et al. (2016) Coproporphyrins in Plasma and Urine Can Be Appropriate Clinical Biomarkers to Recapitulate Drug-Drug Interactions Mediated by Organic Anion Transporting Polypeptide Inhibition. *J Pharmacol Exp Ther* **358**:397–404.

Landrier JF, Eloranta JJ, Vavricka SR, and Kullak-Ublick GA (2006) The nuclear receptor for bile acids, FXR, transactivates human organic solute transporter-alpha and -beta genes. *Am J Physiol Gastrointest Liver Physiol* **290**:G476–G485.

Le Vee M, Gripon P, Stieger B, and Fardel O (2008) Down-regulation of organic anion transporter expression in human hepatocytes exposed to the proinflammatory cytokine interleukin 1beta. *Drug Metab Dispos* **36**:217–222.

Le Vee M, Lecureur V, Stieger B, and Fardel O (2009) Regulation of drug transporter expression in human hepatocytes exposed to the proinflammatory cytokines tumor necrosis factor-alpha or interleukin-6. *Drug Metab Dispos* **37**:685–693.

Lee H, Zhang Y, Lee FY, Nelson SF, Gonzalez FJ, and Edwards PA (2006) FXR regulates organic solute transporters alpha and beta in the adrenal gland, kidney, and intestine. *J Lipid Res* **47**:201–214.

Lu TT, Makishima M, Repa JJ, Schoonjans K, Kerr TA, Auwerx J, and Mangelsdorf DJ (2000) Molecular basis for feedback regulation of bile acid synthesis by nuclear receptors. *Mol Cell* **6**:507–515.

Maeda K (2015) Organic anion transporting polypeptide (OATP)1B1 and OATP1B3 as important regulators of the pharmacokinetics of substrate drugs. *Biol Pharm Bull* **38**:155–168.

Meyer Zu Schwabedissen HE, Böttcher K, Chaudhry A, Kroemer HK, Schuetz EG, and Kim RB (2010) Liver X receptor α and farnesoid X receptor are major transcriptional regulators of OATP1B1. *Hepatology* **52**:1797–1807.

Meyer zu Schwabedissen HE and Kim RB (2009) Hepatic OATP1B transporters and nuclear receptors PXR and CAR: interplay, regulation of drug disposition genes, and single nucleotide polymorphisms. *Mol Pharm* **6**:1644–1661.

Niemi M (2007) Role of OATP transporters in the disposition of drugs. *Pharmacogenomics* **8**:787–802.

Niemi M, Pasanen MK, and Neuvonen PJ (2011) Organic anion transporting polypeptide 1B1: a genetically polymorphic transporter of major importance for hepatic drug uptake. *Pharmacol Rev* **63**:157–181.

Nishimura M, Koeda A, Shimizu T, Nakayama M, Satoh T, Narimatsu S, and Naito S (2008) Comparison of inducibility of sulfotransferase and UDP-glucuronosyltransferase mRNAs by prototypical microsomal enzyme inducers in primary cultures of human and cynomolgus monkey hepatocytes. *Drug Metab Pharmacokinet* **23**:45–53.

Oswald M, Kullak-Ublick GA, Paumgartner G, and Beuers U (2001) Expression of hepatic transporters OATP-C and MRP2 in primary sclerosing cholangitis. *Liver* **21**:247–253.

Pai R, French D, Ma N, Hotzel K, Plise E, Salphati L, Setchell KD, Ware J, Lauriault V, Schutt L, et al. (2012) Antibody-mediated inhibition of fibroblast growth factor 19 results in increased bile acids synthesis and ileal malabsorption of bile acids in cynomolgus monkeys. *Toxicol Sci* **126**:446–456.

Peyer AK, Jung D, Beer M, Gnerre C, Keogh A, Stroka D, Zavolan M, and Meyer UA (2007) Regulation of human liver delta-aminolevulinic acid synthase by bile acids. *Hepatology* **46**:1960–1970.

Ponka P (1999) Cell biology of heme. *Am J Med Sci* **318**:241–256.

Qin P, Borges-Marcucci LA, Evans MJ, and Harnish DC (2005) Bile acid signaling through FXR induces intracellular adhesion molecule-1 expression in mouse liver and human hepatocytes. *Am J Physiol Gastrointest Liver Physiol* **289**:G267–G273.

Qiu X, Bi YA, Balogh LM, and Lai Y (2013) Absolute measurement of species differences in sodium taurocholate cotransporting polypeptide (NTCP/Ntcp) and its modulation in cultured hepatocytes. *J Pharm Sci* **102**:3252–3263.

Rodrigues AD, Lai Y, Shen H, Varma MVS, Rowland A, and Oswald S (2020) Induction of Human Intestinal and Hepatic Organic Anion Transporting Polypeptides: Where Is the Evidence for Its Relevance in Drug-Drug Interactions? *Drug Metab Dispos* **48**:205–216.

Rodrigues AD, van Dyk M, Sorich MJ, Fahmy A, Useckaite Z, Newman LA, Kapetas AJ, Mounzer R, Wood LS, Johnson JG, et al. (2021) Exploring the Use of Serum-Derived Small Extracellular Vesicles as Liquid Biopsy to Study the Induction of Hepatic Cytochromes P450 and Organic Anion Transporting Polypeptides. *Clin Pharmacol Ther* **110**:248–258.

Shen H, Dai J, Liu T, Cheng Y, Chen W, Freeden C, Zhang Y, Humphreys WG, Marathe P, and Lai Y (2016) Coproporphyrins I and III as Functional Markers of OATP1B Activity: In Vitro and In Vivo Evaluation in Preclinical Species. *J Pharmacol Exp Ther* **357**:382–393.

Shitara Y, Maeda K, Ikejiri K, Yoshida K, Horie T, and Sugiyama Y (2013) Clinical significance of organic anion transporting polypeptides (OATPs) in drug disposition: their roles in hepatic clearance and intestinal absorption. *Biopharm Drug Dispos* **34**:45–78.

Slijepcevic D, Roscam Abbing RLP, Katafuchi T, Blank A, Donkers JM, van Hoppe S, de Waart DR, Tolenaars D, van der Meer JHM, Wildenberg M, et al. (2017) Hepatic uptake of conjugated bile acids is mediated by both sodium taurocholate cotransporting polypeptide and organic anion transporting polypeptides and modulated by intestinal sensing of plasma bile acid levels in mice. *Hepatology* **66**:1631–1643.

Song KH, Li T, Owsley E, Strom S, and Chiang JY (2009) Bile acids activate fibroblast growth factor 19 signaling in human hepatocytes to inhibit cholesterol 7alpha-hydroxylase gene expression. *Hepatology* **49**:297–305.

van de Wiel SMW, Bijsmans ITGW, van Mil SWC, and van de Graaf SFJ (2019) Identification of FDA-approved drugs targeting the Farnesoid X Receptor. *Sci Rep* **9**:2193.

Zhang J, Yasuda M, Desnick RJ, Balwani M, Bishop D, and Yu C (2011) A LC-MS/MS method for the specific, sensitive, and simultaneous quantification of 5-aminolevulinic acid and porphobilinogen. *J Chromatogr B Analyt Technol Biomed Life Sci* **879**:2389–2396.

Zhang Y, Chen C, Chen SJ, Chen XQ, Shuster DJ, Puszczalo PD, Fancher RM, Yang Z, Sinz M, and Shen H (2020) Absence of OATP1B (Organic Anion-Transporting Polypeptide) Induction by Rifampin in Cynomolgus Monkeys: Determination Using the Endogenous OATP1B Marker Coproporphyrin and Tissue Gene Expression. *J Pharmacol Exp Ther* **375**:139–151.

Zollner G, Fickert P, Zenz R, Fuchsbichler A, Stumptner C, Kenner L, Ferenci P, Stauber RE, Krejs GJ, Denk H, et al. (2001) Hepatobiliary transporter expression in percutaneous liver biopsies of patients with cholestatic liver diseases. *Hepatology* **33**:633–646.

Address correspondence to: Dr. Hong Shen, Scientific Director, Drug Metabolism and Pharmacokinetics (DMPK) Department, Pharmaceutical Candidate Optimization (PCO), Bristol Myers Squibb Company (BMS), Route 206 & Province Line Road, Princeton, NJ 08543. E-mail: hong.shen1@bms.com

Supplementary Figures

Repression of OATP1B Expression and Increase of Plasma Coproporphyrin Level as Evidence for OATP1B Down-regulation in Cynomolgus Monkeys Treated with Chenodeoxycholic Acid

Yueping Zhang, Shen-Jue Chen, Cliff Chen, Xue-Qing Chen, Sagnik Chatterjee, David J. Shuster, Heather Dexter, Laura Armstrong, Elizabeth M. Joshi, Zheng Yang, and Hong Shen

Supplementary Figure 1
Mean plasma concentrations of LCA (A), CA (B), and DCA (C) before (Day -4 and Day -2), during (Day 1 to Day 8), and one day after (Day 9) administration of CDCA (50 and 100 mg/kg/day) in three male cynomolgus monkeys. Data are shown as the mean and SD values.

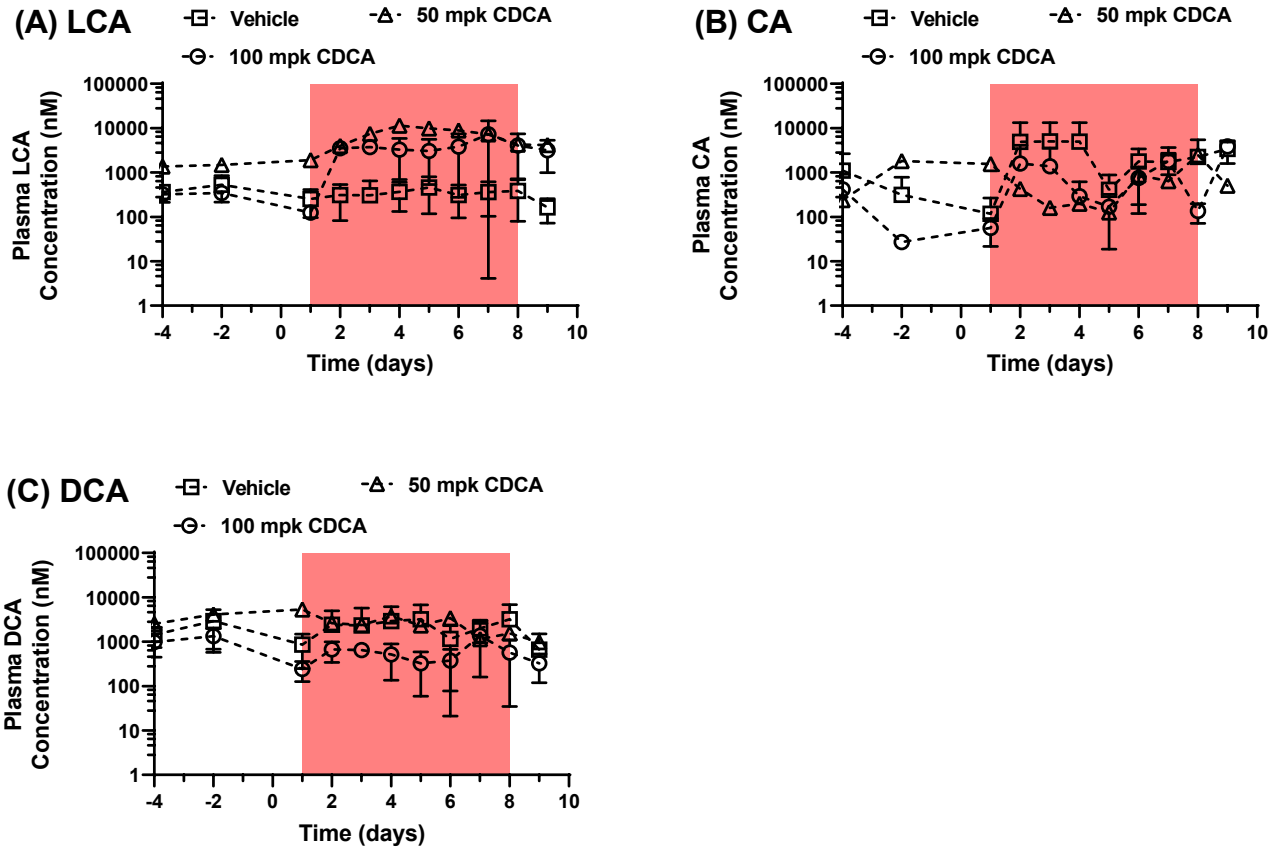

Supplementary Figure 2
Mean plasma concentrations of LCA (A), CA (B), and DCA (C) on Day 1 after the first vehicle (blue closed squares), 50 mpk CDCA (red closed triangles), or 100 mpk CDCA dose (black closed circles), and on Day 8 after the eighth vehicle (blue open squares), 50 mpk CDCA (red open triangles), or 100 mpk CDCA dose (black open circles) are shown as mean and SD values.

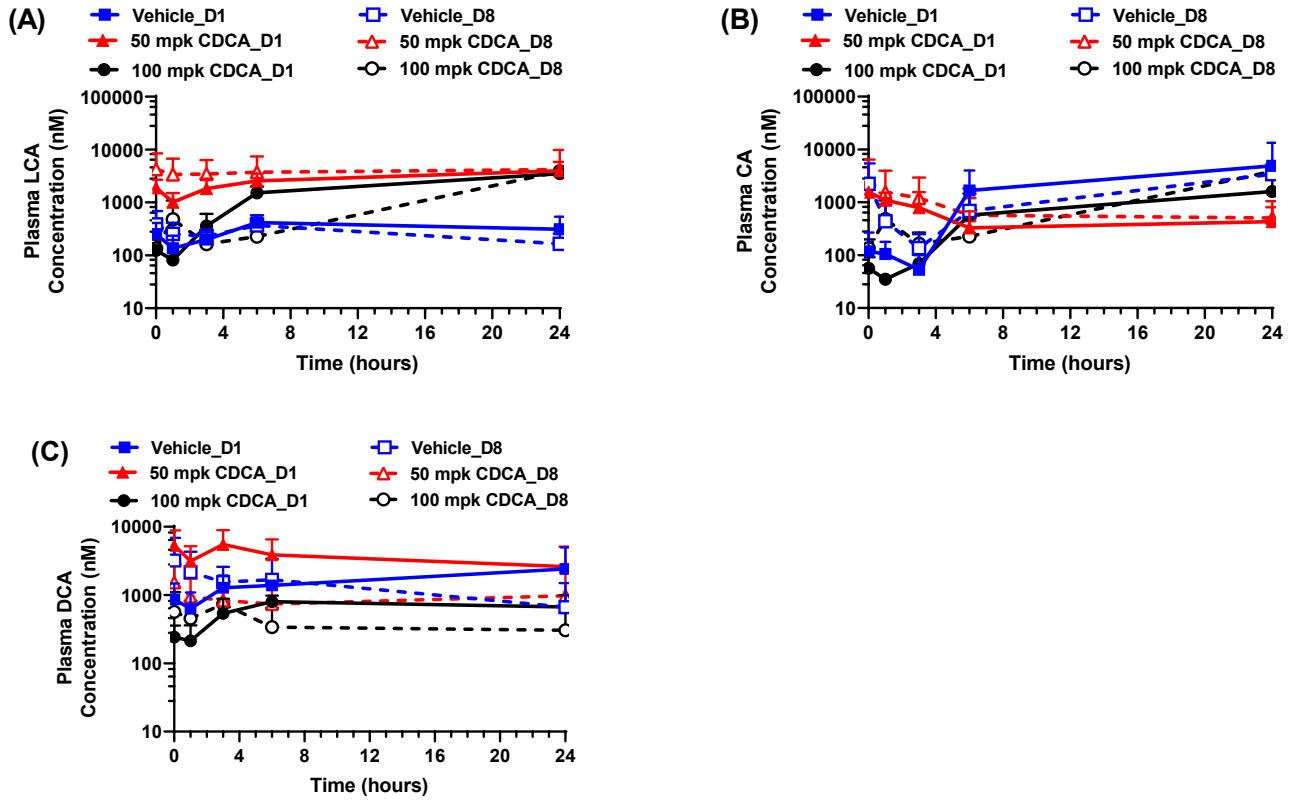

Supplementary Figure 3

Effects of CDCA and RIF treatments on the liver concentrations of CPI (A), CPIII (B), CDCA (C), LCA (D), CA (E), and DCA (F) of cynomolgus monkeys. The animals were treated with vehicle (blue bars), CDCA (50 and 100 mg/kg; red and black bars, respectively), or RIF (15 mg/kg; grey bars) once daily for 8 days. Data are expressed as mean and SD values from 3 to 6 monkeys. Statistics were conducted by t-test. *p < 0.05 was significantly different compared to vehicle controls.